Comparison between Grid-Tied Phase Current Control Implemented Under Stationary $0\alpha\beta$ and Natural Reference Frames

Ricardo L. A. Ribeiro†, Rafael R. Aquino*, Carlos M. C. Filho†, Thiago O. A. Rocha†
*Programa de Pós-Graduação em Engenharia Elétrica e de Computação
†Departamento de Engenharia Elétrica
Universidade Federal do Rio Grande do Norte
Email: rlucio@ct.ufrn.br†, rafaelribeirorraquinho@gmail.com*, carlosmchesterf@gmail.com*,
thiago.rocha@ct.ufrn.br†

***Abstract*—The growing demand for energy has increased the use of renewable sources, like wind power and photovoltaic. These systems interconnect the power grid via grid-tied voltage source inverters. Generally, they are inserted in three-phase networks that can be configured three-wire or four-wire systems. The four-wire networks could operate under unbalanced conditions which address to non-standard control approaches for regulating the grid-tied output currents. This work presents a comparison study for the implementation of those phase current control strategies under $0\alpha\beta$ or natural reference frames. Moreover, the proposed works discuss how to determine the suitable reference currents under both referential frames for accomplishing the required system energy balance. Simulation results obtained from a three-phase grid-tied system validates the proposed comparison evaluation.**

***Keywords* – renewable source, voltage source inverters, three-wire three-phase system, four-wire three-phase system, current control**

I. Introduction

The renewable energies, such as wind power and solar energy, have seen a rapid increase as distributed generation (DG) in the last few years in order to decrease carbon emissions. Moreover, the substitution of concentrated generation concept for the DG system introduces many advantages, such as lower power loss due to the reduction of transmission lines length, robustness, and superior reliability.

Generally, these DG systems based on renewable sources interconnect to the power grid via grid-tied power inverters, actually denominated of active front ends. These power converters employ dedicated control strategies for regulating the power flow from the DG to the mains. The control mentioned above uses the multi-loop configuration in which the outer loop regulate the active and reactive power flow and the inner control loops of the DG output currents. These DG systems could be composed of single-phase or three-phase sources. When most of the DG are single-phase sources, unbalanced operation conditions can be verified in the microgrid. This asymmetry could result in voltage oscillations and electrical losses that can affect the power system stability.

Three-phase four-wire power conversion topologies have been proposed to address the control issues demanded by the unbalanced systems. These converters are composed of four legs in which the fourth leg interconnects the neutral terminal of the Point of Common Coupling (PCC). This configuration inserts an additional degree of freedom, despite the cost increase determined by the power switches and gate drive circuits [1], [2].

Control standard techniques can regulate the output phase current of the DG implemented by using the grid-tied four-leg converter following the stationary reference frame ($0\alpha\beta$) or synchronous reference frame ($0dq$) [4]. However, these choices demand complex issues to determine the reference currents for achieving the required energy balance on unbalanced conditions. An alternative is to employ current controllers in each system phase to accomplish both requirements. In this case, proportional-resonant controllers (PR) can overcome the drawbacks mentioned above [3]. This control strategy permits the definition of suitable reference signals based on the energy balance of each system phase.

Three-phase four-wire grid-connect converter has been recommended as the most suitable topology for operating under unbalanced conditions [4], [5], [6]. The connection of the neutral wire to the converter fourth leg provides an extra freedom degree and permits to control the neutral current [7] and decoupling the system phases [8]. Therefore, the four-wire system can be treated as three single-phase independent circuits. Moreover, the current of these single-phase circuits can be controlled individually by suitable regulators, which reduces the complexity of implementation, as shown in [9].

This paper proposes a comparison study for evaluating the current control applied for the unbalanced system implemented under stationary $0\alpha\beta$ or natural (abc) reference frames. The evaluation of both control strategies employs power quality issues based on total harmonic distortion and system unbalance index [11]. Besides, the proposed study also evaluates two possible methods for generating the grid-tied reference for unbalanced conditions. In the first, the amplitude of the current reference vector is determined, with the phase current

references defined with the same amplitude. In the second, the reference currents of each decoupled single-phase circuit are determined proportionally to the respective grid phase voltage, emulating a resistive load. Simulations studies obtained from a grid-tied converter, based on four-wire systems validate the proposed comparative study.

II. System description and modelling

Fig. 1 presents the grid-tied of the power converter topology employed in this study. It comprises a four-leg voltage source converter (VSC) interconnected to a four-wire power grid via filter inductance $L_{f,x}$ $(x = \{a, b, or\ c\})$. In this diagram, the power grid is composed of three ideal sinusoidal voltage sources, series interconnected with their respective internal impedance $Z_{\{}g, x\}$ $(x = \{a, b, or\ c\})$. The neutral wire is also modelled by an internal impedance $Z_{\{}g, n\}$. This converter topology permits that each system phase can be treated as equivalent single-phase circuits, as shown in Fig. 2 for the phase a of the power grid.

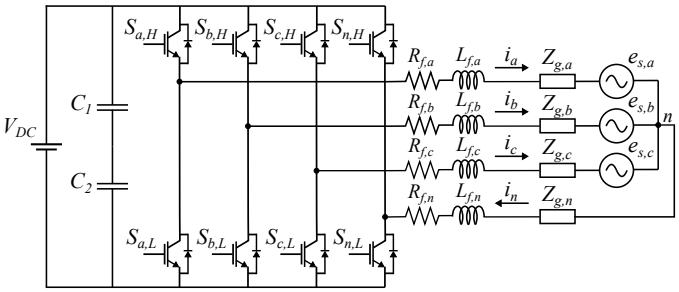

Fig. 1. Three-phase grid-tied system based on four-wire VSC.

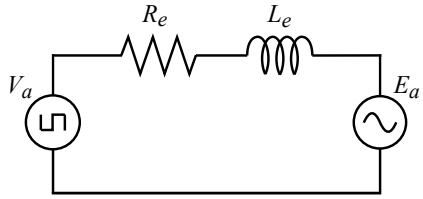

Fig. 2. Single-phase equivalent circuit of the four-wire grid-tied system.

The four-wire grid-tied converter is interconnected to the power grid via L-filters, represented by the series association of filter inductance L_f and their inherent resistance R_f (i.e., $R_f + j\omega L_f$). Therefore, the equivalent impedance that results by the series association between interconnection filter and internal grid impedance (i.e., $R_g + jwL_g$) can be represented by a series association of equivalent resistance Re and equivalent inductance Le (i.e., $R_e + j\omega L_e$). Fig 2 presents the single-phase equivalent circuit of the grid-tied four-wire converter. Kirchhoff's voltage law applied for the equivalent circuit presented in Fig. 2, determines the single-phase dynamic model of the grid-tied four-wire system, that can be given by

$$V_a - E_s = R_e i_s + L_e \frac{di_s}{dt} \tag{1}$$

By applying the Laplace Transform to the Eq. (1), the dynamic model can be rewritten as

$$V_a(s) - E_s(s) = (R_e + sL_e)I_s(s) \tag{2}$$

Therefore, the transfer function related to grid-tied output currents can be obtained from the Eq. (2), which results in

$$I_s(s) = \frac{\frac{1}{L_e}}{s + \frac{R_e}{L_e}} V_a(s) - \frac{\frac{1}{L_e}}{s + \frac{R_e}{L_e}} E_s(s) \tag{3}$$

In which, the first term of Eq. (3) represents the transfer function of the grid-tied output single-phase current Is, imposed by the VSC. The second term of Eq. (3) refers to a disturbance introduced by the power grid that must be compensated by the current regulator.

III. Control System

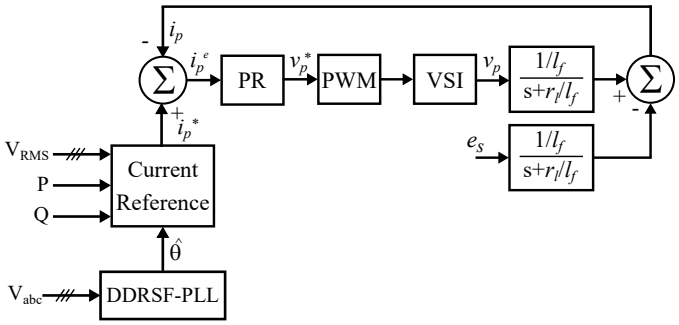

Fig. 3. Block diagram of the current control loop implemented on natural reference frame.

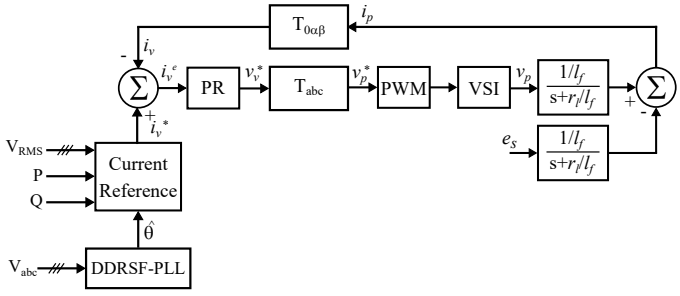

Fig. 4. Block diagram of the current control loop implemented on $0\alpha\beta$ stationary reference frame.

Figs. 3 and 4 present the block diagrams of the control strategy employed for regulating the output currents of the four-wire grid-tied systems. Fig 3 presents the block diagram of the grid-tied output current control strategy implemented on the natural reference frame (i.e., each grid-tied phase is controlled individually). Fig 4 depicts the block diagram of the control strategy implemented on the stationary reference frame (i.e., $0\alpha\beta$ reference frame). Both control systems employ a Decoupled Double Synchronous Reference Frame Phase-Locked Loop (DDSRF-PLL) for generating the reference

frame aligned to the power grid voltage vector. Proportional-Resonant (PR) Controllers regulate the grid-tied output currents of both structures.

In the Fig. 3, the index p represents each grid-tied phase (i.e., $p = \{a, b, c\}$) in which each phase is controlled individually. While in Fig. 4, the output currents of grid-tied systems are regulated on the stationary reference frame, and index v refers to the $0\alpha\beta$ phase currents (i.e., $v = \{0, \alpha, \beta\}$). The Current Reference block generates suitable reference currents based on power grid voltage amplitude and active and reactive power for accomplishing the system energy balance.

A. Current Reference System

For providing appropriate reference currents, initially, the average value of root-mean-square (RMS) of the power grid voltage is determined as

$$\overline{V_{RMS}} = \frac{V_{a(RMS)} + V_{b(RMS)} + V_{c(RMS)}}{3} \tag{4}$$

The average value, given by the Eq. (4), is used together with the active and reactive powers for determining suitable values of grid-tied reference currents.

The apparent power drawn by the four-wire grid-tied system is given by

$$|S| = \sqrt{P^2 + Q^2} \tag{5}$$

Therefore, the average value of the grid-tied output current ($\overline{I_{RMS}}$) can be determined as

$$\overline{I_{RMS}} = \frac{|S|}{\overline{V_{RMS}}} \tag{6}$$

The amplitude of each phase current of the grid-tied can be obtained as follows. A proportional factor is determined by dividing the RMS voltage amplitude of each phase by the RMS average value determined by Eq. (4). This proportional factor is multiplied by the RMS average value of the system current obtain by Eq. (5), multiplying by $\sqrt{2}$ for achieving the amplitude value of each system phase. Finally, the displacement between each phase voltage and the phase current is inserted by using the power factor angle (φ). Therefore, the reference current of the grid-tied phase a is given by

$$i_a^*(t) = \frac{V_{a(RMS)}}{\overline{V_{RMS}}} \overline{I_{RMS}} \sqrt{2} \angle(\theta(t) + \varphi) \tag{7}$$

Where $\theta(t)$ is the angle of the voltage vector estimated by the DDSRF-PLL. In the case of the control strategy implemented on the stationary reference frame, the phase $0\alpha\beta$

reference currents can be obtained from the Clark Transform matrix from the values obtained by using Eq. (7).

B. Decoupled Double Synchronous Reference Frame Phase-Locked Loop

The knowledge of the voltage vector angle is essential for implementing the grid-tied output current control loop. Moreover, applications with four-wire networks suffer from possible unbalance conditions that could result in negative sequence currents. Therefore, it is necessary to employ a PLL with a suitable structure for extracting the positive sequence of the power grid voltage measurements. Conventional PLLs like SRF-PLL can generate undesired angle deviations under unbalanced conditions. The reduction of the bandwidth of the SRF-PLL controller can mitigate this drawback but introduces undesired delays, which can cause angle estimation mismatches.

The use of decoupled double synchronous reference frame phase-locked loop (DDSRF-PLL) can overcome the drawbacks mentioned before [10]. The DDSRF-PLL extracts both positive and negative sequences separately. Therefore, it is possible to generate well-suited reference currents by using only positive-sequence information of the voltage measurements.

Figs. 5 and 6 present the estimated angle of an unbalanced power grid obtained from SRF-PLL or DDSRF-PLL. Fig. 5 depicts the voltage phase waveforms of a three-phase unbalance power grid. The unbalanced condition of this power grid was obtained by increasing the 30% voltage amplitude of phase a. Fig. 6 presents the voltage vector angles obtained via both PLL structures. In this graph, the red line refers to the phase angle obtained by using a standard SRF-PLL while the blue line corresponds to the phase angle estimated via the DDSRF-PLL. This graph demonstrates that the voltage vector angle obtained through the DDSRF-PLL is superior in comparison to the SRF-PLL.

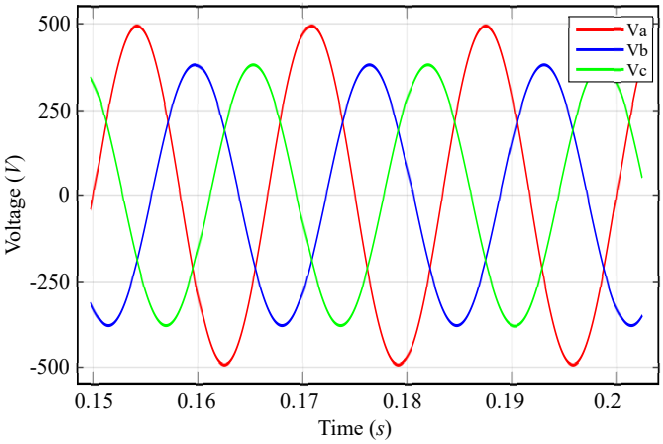

Fig. 5. Voltages waveforms of the unbalanced power grid.

C. Proportional-Resonant Controller

Both control strategies employ PR controllers for regulating their output phase currents [4], which transfer function of the PR controller can be given by [4]

$$G_c(s) = K_p + K_I \frac{s}{s^2 + \omega^2} \tag{8}$$

where K_p and K_i are the proportional and integral control gains.

The main difference in comparison to the conventional standard proportional-integral (PI) controller refers to the insertion

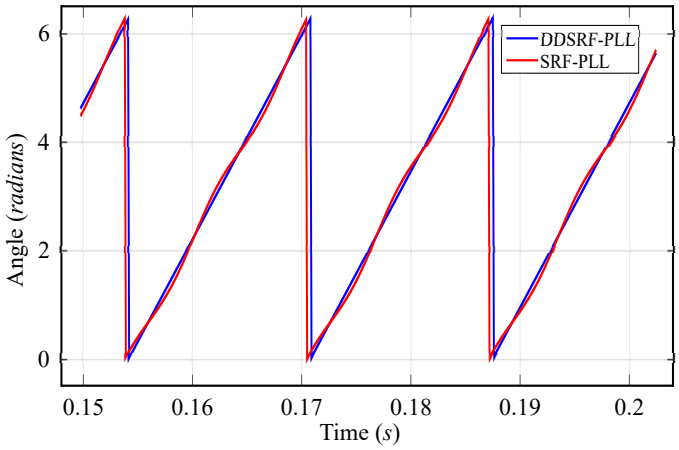

Fig. 6. Voltage vector phase angle obtained from SRF-PLL and DDSRF-PLL.

of the internal model of sinusoidal reference, which results in the integral term represented by the second parcel of Eq. (8).

D. Design Criteria of the PR Controllers

The design approach used for determining the controller gains is based on the pole placement control (PPC) technique. From the grid-tied transfer function of Eq. (3), neglecting the disturbance term, the closed-loop transfer function of the grid-tied output current can be expressed as

$$G_f(s) = \frac{\frac{1}{L_e}(sK_p + K_i)}{s^2 + (\frac{R_e + K_p}{L_e}) + \frac{K_i}{s}} \tag{9}$$

The closed-loop transfer function of the grid-tied four-wire system given by Eq. (9) is a second-order type. Therefore, the characteristic polynomial that describes the dynamic behavior of second-order systems can be given by

$$P(s) = s^2 + 2\xi\omega_n + \omega_n^2 \tag{10}$$

where ξ is the damping coefficient and ω_n is the natural frequency.

The controller gains Kp e Ki can be obtained by solving the Diophantine equation from Eqs (9) and (10). Based on this design control technique, the controller gains can be given by

$$K_i = L_e\omega_n^2 \tag{11}$$

$$K_p = 2L_e\xi\omega_n - R_e \tag{12}$$

Take into account the transfer function of Eq. (3) and applying the system specifications presented in Tab. I, the setup parameters of the characteristic polynomial of Eq. (10) can be defined by $\omega_n = 1885rad/s$ and $\xi = 0.707$. This setup parameters address to the required performance of the grid-tied four-wire system. By using the Eqs. (11)- (12), the controller gains obtained for this design criterion are $K_p = 2.266$ and $K_i = 3553.1$.

P	$2.8kW$
l_f	$1mH$
r_f	0.4Ω
l_g	$400\mu H$
r_g	0.4Ω
f_s	$10kHz$
V_dc	$450V$

TABLE I
PARAMETERS OF THE SIMULATION SETUP DEPICTED IN FIG. 1.

IV. SIMULATION RESULTS

A simulation program accomplished the performance of both control strategies via PSIM, based on the system presented in Fig. 1, controlled according to the block diagrams of Fig. 3 and 4. Tab. 1 presents the parameters of the simulation setup.

The suitable reference current of each phase of the grid-tied power converter is generated based on the active and reactive powers required for achieving the system energy balance and taking account of the value of voltage amplitude. Therefore, under the unbalanced condition, each current phase can be imposed individually proportionally to each grid voltage. This approach overcomes the drawbacks verified for defining well-suited reference currents for unbalanced systems.

The output currents of the grid-tied four-leg power converter are imposed by PR controllers implemented on the stationary reference frame ($0\alpha\beta$) or natural frame (abc). In the case of $0\alpha\beta$ implementation, the PR controllers synthesize the reference voltages on the same reference frame that are transformed to the natural reference frame abc. Both implementations employ a sinusoidal pulse width modulation for generating the commands of the converter switches.

The conventional solution employs balanced reference currents with an amplitude of $10A$. The condition above was applied for the four simulation results, with balanced and unbalanced conditions. The unbalanced condition was emulated with phase voltage given by $V_a = 1.1V_b$, $V_c = 0.9V_b$ and $V_b = 127\ V(rms)$. The control approach that emulates the resistive behavior, the reference currents are generated proportionally to its respective phase voltage, which results in $I_a = 11\ A$, $I_b = 10\ A$ and $I_c = 9\ A$.

Fig. 7 presents the graphs of the grid phase voltages waveforms under the unbalance conditions described above. Fig. 8 depicts the simulation results of the conventional control approach in which the amplitudes of the reference currents are determined with the same amplitude despite the unbalance conditions of the power grid.

Fig. 9 depicts the simulation results of controlled phase currents imposed by using the resistive emulation according to the proposed method described by Eqs. (4)-(7). Differently from the results presented in Fig. (8), the grid-tied output phase currents present different amplitudes that are proportional to the respective grid phase voltage amplitude. This simulation demonstrates the effectiveness of the proposed method in emulating an equivalent resistive behavior of the grid-tied system.

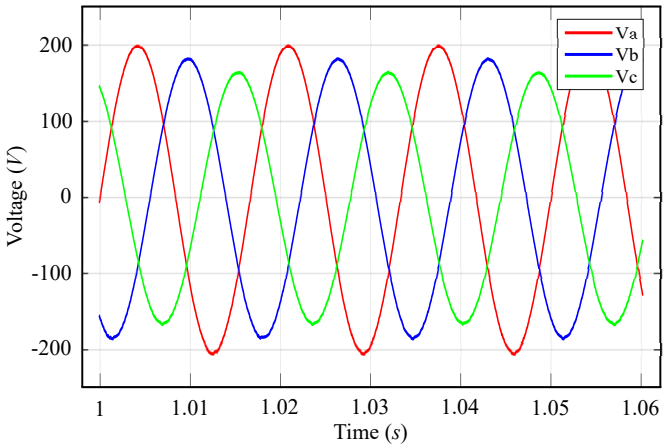

Fig. 7. Voltage waveforms of the unbalanced power grid.

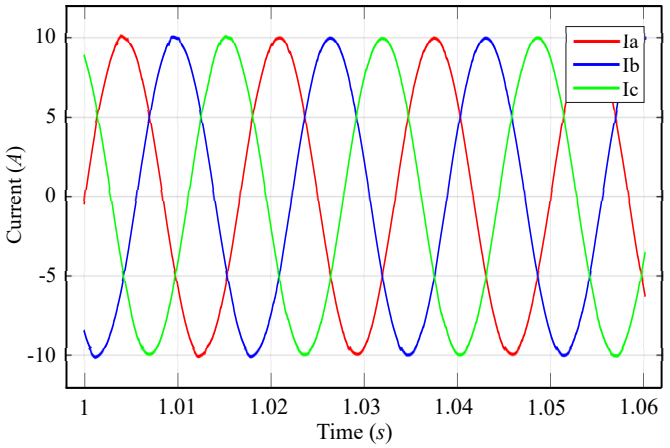

Fig. 8. Phase current waveform obtained by using the standard control strategy

Table II presents the THD of the phase currents related to the simulations presented before. It is possible to observe that the control strategy implemented on the natural reference frame provides phase currents with smaller THD in comparison to the control approach implemented in the stationary reference frame. Despite the smaller THD shown in the resistive emulator approach, it presents the disadvantage due to the presence of the inherent neutral current generated by the unbalanced condition. The presence of the neutral current in the grid-tied system could increase the system losses, and this must be a trade-off to be considered in the choice of the grid-tied control approach.

V. Conclusion

This work presented a comparison between two control approaches for regulating output currents of DGs implemented by four-wire converters applied for four-wire networks. Even though both control strategies are similar, the control approach that emulates the resistive behavior for generating the phase reference currents, individually, demonstrated to have better performance, with reduced THD. However, resistive behavior can produce important issues related to the presence of neutral

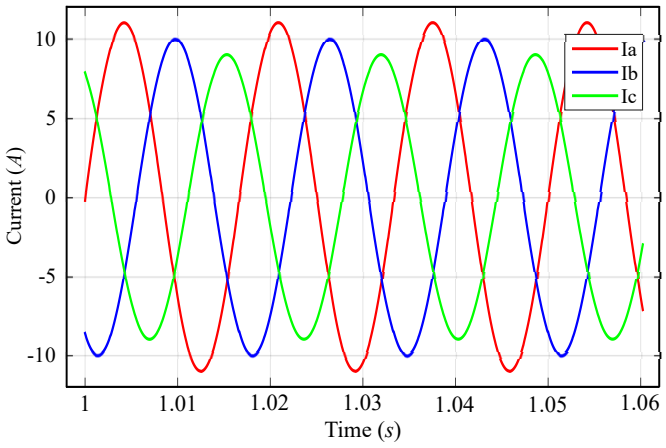

Fig. 9. Phase current waveform obtained by using the *abc* control strategy.

THD	$0\alpha\beta$ conv.	$0\alpha\beta$ res.	per phase conv.	per phase res.
Ia	0.5574%	0.2907%	0.5145%	0.2530%
Ib	0.5595%	0.5242%	0.4930%	0.4708%
Ic	0.5740%	0.3840%	0.5116%	0.3217%
$\overline{I}$	0.5636	0.3996	0.5283	0.3485
Va	0.2787%	0.2503%	0.2834%	0.2555%
Vb	0.2718%	0.2946%	0.2662%	0.2856%
Vc	0.2617%	0.2682%	0.2685%	0.2665%
$\overline{V}$	0.2707	0.2710	0.2727	0.2692

TABLE II
THD OBTAINED FROM THE SIMULATION OF CONTROL STRATEGIES OF BLOCK DIAGRAMS OF FIGS 3 AND 4.

current, which could result in increased system losses in comparison with the standard solution.

Acknowledgment

To Laboratório de Eletrônica Industrial e Energias Renováveis (LEIER-UFRN).

References

[1] Y. Li, D. M. Vilathgamuwa, and P. C. Loh, *Microgrid power quality enhancement using a three-phase four-wire grid-interfacing compensator*, IEEE Trans. Ind. Appl., vol. 41, no. 6, pp. 1707–1719, Nov. 2005.

[2] R. R. Sawant and M. C. Chandorkar, *A multifunctional four-leg grid-connected compensator*, IEEE Trans. Ind. Appl., vol. 45, no. 1, pp. 249–259, Jan. 2009.

[3] D. N. Zmood and D. G. Holmes, *Stationary frame current regulation of PWM inverters with zero steady-state error*, IEEE Trans. Power Electron., vol. 18, no. 3, pp. 814–822, May 2003.

[4] Remus Teodorescu, Frede Blaabjerg, *Proportional-Resonant Controllers. A New Breed of Controllers Suitable for Grid-Connected Voltage-Source Converters* , Journal of Electrical Engineering.

[5] E. dos Santos, C. Jacobina, N. Rocha, J. Dias, and M. Correa, *Single-Phase to three-phase four-leg converter applied to distributed generation system*, IET Power Electron., vol. 3, no. 6, pp. 892–903, Nov. 2010.

[6] R. M. Mohammad, F. R. Mohd, A. G. Ali, and W. M. Mohd, *Control techniques for three-phase four-leg voltage source inverters in autonomous microgrids: A review*, Renew. Sustain Energy Rev., vol. 54, pp. 1592–1610, 2016.

[7] M. Rivera, V. Yaramasu, A. Llor, J. Rodriguez, B. Wu, and M. Fadel, *Digital predictive current control of a three-phase four-leg inverter*, IEEE Trans. Ind. Electron., vol. 60, no. 11, pp. 4903–4912, Nov. 2013.

[8] R. Zhang, V. H. Prasad, D. Boroyevich, and F. C. Lee, *Three-dimensional space vector modulation for four-leg voltage-source converters*, IEEE Trans. Ind. Electron., vol. 60, no. 11, pp. 4903–4912, Nov. 2013. IEEE Trans. Power Electron., vol. 17, no. 3, pp. 314–326, May 2002.

[9] P. H. I. Hayashi and L. Matakas, *Decoupled stationary ABC frame current control of three-phase four-leg four-wire converters*, in Proc. Brazilian Power Electron. Conf., 2017, pp. 1–6.

[10] Pedro Rodrígues, Josep Pou, Joan Bergas, J. Ignacio Candela, Rolando P. Burgos and Dushan Boroyevich, *Decoupled Double Synchronous Reference Frame PLL for Power Converters Control*, IEEE Trans. Power Electron., vol. 22, no. 2, March 2007.

[11] A. Mansour, Zhang Chengning, *Measurement of Power Components in Balanced Three-Phase Systems Under Nonsinusoidal Operating Conditions by Using IEEE Standard 1459-2010 and Fourier Analysis*, 2013 The International Conference on Technological Advances in Electrical, Electronics and Computer Engineering (TAEECE).